Turbulent–nonturbulent interface detector

Valdis Kibens, Leslie S. G. Kovasznay*, and Lawrence J. Oswald†

The University of Michigan, Ann Arbor, Michigan 48104

(Received 2 January 1973; and in final form, 28 May 1974)

An analog circuit is presented for the detection in real time of the turbulent–nonturbulent interface at the free stream edge of turbulent shear flows. The output of the circuit is a square wave whose value is unity when the detector probe is in turbulent flow, and is zero when in nonturbulent flow. The effectiveness of several detection schemes is evaluated. A method for calibrating the detector circuit is given by using a "synthetic," intermittently turbulent simulated signal of known intermittency properties. A circuit for generating the simulated signal is also presented.

I. INTRODUCTION

It is characteristic of turbulent shear flows that an intermittently turbulent zone exists between the fully turbulent flow and the adjoining nonturbulent flow. The intermittent zone varies in extent, and in some flows the entire turbulent region may be only intermittently turbulent. On an instantaneous picture the interface between turbulent and nonturbulent regions is a sharp, often convoluted boundary. The instantaneous position of the interface appears to be nominally Gaussian distributed in several quasiparallel shear flows. Since the first observation of the phenomenon by Corrsin[1] in an axisymmetric heated jet, it has been clear that, in order to measure the properties of intermittently turbulent flows, it is necessary to devise methods to separate the record into turbulent and nonturbulent portions and then average each part separately. The determination of the mean value of a fluctuating quantity is simple electronically, while averaging separately only the turbulent, or alternately only the nonturbulent, portion of a fluctuating signal is more difficult and requires the use of a technique that we termed "conditional sampling and averaging." Progress in the understanding of intermittently turbulent flows has been tied to advances in signal processing methods used for identifying the presence or absence of turbulent flow at a particular time and position in space.

We shall define an intermittency function, $I(t,x,y,z)$, for a fixed position x,y,z in an intermittently turbulent flow field whose value is either zero or unity; it is equal to 1 when the flow is turbulent and zero when it is nonturbulent at that location in that instant. Clearly, $I(t)$ is a random square wave and its mean value is $\gamma(x,y,z)$, the intermittency factor that represents the fraction of time the flow is turbulent at the given location x, y, z. The intermittency function is then the basis to form different kinds of conditional averages.

The first electronic circuit devised for this purpose was developed by Townsend.[2] A circuit based on Townsend's was subsequently used by Corrsin and Kistler.[3] Further adaptations of these circuits have been described for low speed flow by Bradbury[4] and for supersonic flows by Demetriades.[5] Fiedler and Head[6] have made improvements on the circuit used by Corrsin and Kistler and adapted it for optical inputs, as they used smoke to identify turbulent regions for use in a variable pressure gradient boundary layer. An alternate method of forming the intermittency function from digitized records has been developed by Kaplan and Laufer[7] using a large digital computer.

Here we describe a new method for obtaining the intermittency function using an analog circuit. The detection scheme described here makes possible a very precise determination of the turbulent–nonturbulent interface crossing in real time. The detector circuit was designed by using solid-state, integrated circuit modules and after completion it has been extensively tested. It was used in the study of turbulent boundary layers[8] and axisymmetric turbulent wakes.[9]

II. CHOICE OF THE INPUT SIGNAL

Fluid mechanical considerations dictate which particular signal be used to form the intermittency function that offers maximum contrast between the turbulent and nonturbulent regions. Figure 1 shows two signals taken from hot wire probes in a wake. Trace (a) shows the signal from a probe sensitive to u, the streamwise fluctuating velocity. Trace (b) shows another signal taken from a probe sensitive to ω_x, the streamwise vorticity.[10] It is clear that the vorticity signal offers more contrast between the turbulent and nonturbulent regions, and we are better able to make an intuitive decision as to which portion of the signal to call turbulent and which nonturbulent. Another possible choice is a signal proportional to a spatial derivative of u, e.g., du/dr in a wake, or du/dy in a boundary layer, which may be regarded as a significant portion of the vorticity component ω_z. The signal finally selected was that proportional to ω_x, the streamwise component of vorticity. Owing to imperfections in the vorticity sensor construction, however, the signal proportional to ω_x is slightly contaminated by parasitic response of the vorticity sensor to streamwise velocity fluctua-

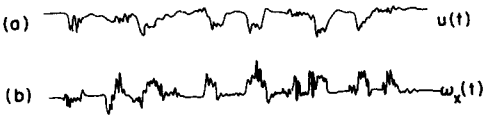

FIG. 1. Oscilllgraph traces of the fluctuating parts of the streamwise velocity, $u(t)$, and of the streamwise vorticity, $\omega_x(t)$, in an axisymmetric wake.

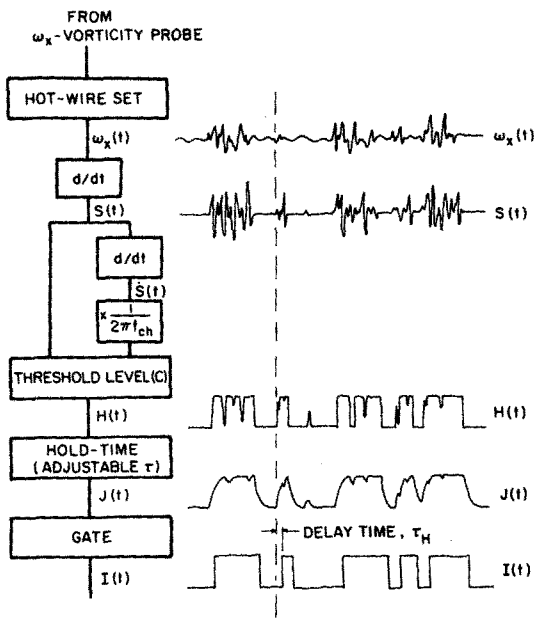

FIG. 2. Block diagram of the detection process and typical waveforms.

tions. This parasitic response results in noticeable low frequency fluctuations in the nonturbulent portions of the signal. To eliminate this low frequency component in the ω_x signal, it was in practice first differentiated with respect to time, so that the input to the detector proper is a signal $S(t)=\partial\omega_x/\partial t$. Further discussion of the reasons for selecting a signal proportional to streamwise vorticity is presented in Sec. VI.

III. DETECTION CRITERIA

In an analog detection scheme only the "past," i.e., the signal up to the present time t, $S(t')$ for $t'<1$, is available as a basis for the desision whether at the present time t, the flow is to be regarded as turbulent or as nonturbulent. The circuit must incorporate a firm, externally imposed set of criteria against which to compare the continuous signal in order to form the intermittency signal $I(t)$ in real time at t or a little later. Linear filtering of the signal $S(t')$ is of course possible and proper filtering may enhance the contrast between the turbulent and nonturbulent portion of the record. An "ideal filter" would be the one that would allow maximum discrimination between the two states. In the following it will be assumed that a near ideal filtering was already performed so that the turbulent and nonturbulent portions of the record are statistically similar, that they have the same power spectrum, and the only difference is in their (rms) signal level. Such an *a priori* notion may be tested, *a posteriori*, by taking conditional zone averages of the fluctuation level; furthermore one may improve the detection by iterating, that is, by first imposing an *a priori* detection criterion, then determining the proper conditional averages and revising the detection criterion, etc.

The specific detection criteria proposed here involved two adjustable parameters. The first of these was a threshold level C. The properly filtered input signal $S(t)$ is characterized by alternately high and low amplitude fluctuations. Intuitively we regard the high intensity portions in $S(t)$ as turbulent periods and the low intensity periods as background noise corresponding to the nonturbulent portion of the record. The threshold C must be adjusted to an appropriate level so that our intuitive notions will correspond to the decision by the circuit as turbulent and nonturbulent states. Clearly the value of C must lie somewhere between S_T', the rms value of the signal $S(t)$ in the turbulent portion, and S_{NT}' in the nonturbulent portion. A reasonable choice can be made, e.g., by setting $C=(S_T'S_{NT}')^{\frac{1}{2}}$, if we assume that S_T' and S_{NT}' are known *a priori*.

The other adjustable parameter is a time constant, the "hold-time," τ_H, that represents the length of the time interval over which the threshold criterion is applied, in the sense that the intermittency function will not change state for short events of duration less than τ_H. In other words, if the level of $S(t)$ drops below C for a short interval less than τ_H there will be no temporary "lapse" in $I(t)$ and it will remain unity. Similarly, occasional "spikes" lasting less than τ_H will not cause a change from 0 to 1 in $I(t)$ during a nonturbulent portion of the record. An inherent effect of introducing the hold-time is that the intermittency function $I(t)$ will lag the actual interface crossing time by a detection delay time which is proportional to τ_H. The hold-time must be chosen according to the characteristic time scale associated with the fine structure of the turbulence within the turbulent region. A characteristic time scale of the turbulent region may be determined most conveniently by examining the properties of turbulence within the interior of the flow where the intermittency factor has reached the value unity. Here we use the tacit assumption that the spectrum and other statistical properties of the turbulent region are the same all across the intermittent zone. One may define the characteristic time T_{ch} or characteristic frequency $f_{ch}=T_{ch}^{-1}$ by comparing the rms value of $S(t)$ and its time derivative $\dot{S}(t)$.

$$\dot{S}'=2\pi f_{ch}S'=2\pi S'/T_{ch}, \tag{1}$$

where $\dot{S}=dS(t)/dt$. The value of the hold-time, τ_H, must be chosen proportional to T_{ch}, but the final choice must be determined on the basis of the best match of the detector output $I(t)$ with our intuitive notion of the "correct" output, or improved choices may be obtained by iteration. We should note that the time scale derived according to Eq. (1) is based on the comparison of the 1st and 2nd derivatives of the signal proportional to the streamwise vorticity fluctuations. The choice of an input function proportional to some other fluctuating turbulent quantity is likely to give a different value for a time scale of the fine structure for the same turbulent flow.

The signal $S(t)$ may be thought of as consisting of a turbulent portion, $B(t)$, having an rms value b, and a nonturbulent portion, $N(t)$, with an rms value n. Therefore $S(t)=I(t)B(t)+[1-I(t)]N(t)$. Naturally, the detection process would improve as the ratio b/n increases, and we shall refer to the ratio b/n as the signal-to-noise ratio, or the quantity that controls detection efficiency.

IV. THE CHOICE OF DETECTOR PARAMETERS

Figure 2 shows a block diagram of the detector and the method used for introducing the parameters C and τ_H. First

an intermediate function $H(t)$ was formed,

$$H(t)=\begin{cases}0 \text{ when } |S|<C \text{ and } (1/2\pi f_{ch})|\dot{S}|<C \\ 1 \text{ when } |S|\geq C \text{ or } (1/2\pi f_{ch})|\dot{S}|\geq C.\end{cases} \quad (2)$$

This definition amounts to the statement that $H=1$ whenever the instantaneous absolute value of either the function S or its time derivative $\dot{S}$ exceeds a prescribed limit.

The motivation for selecting a double criterion to form the function $H(t)$ is demonstrated most easily if we consider an idealized situation. Let the signal $S(t)$ be a sine wave of frequency f_{ch} whose amplitude is alternating between two levels corresponding to turbulent and nonturbulent portions of the signal $S(t)$. The requirement $|S|\geq C$ produces a function $H_1(t)$ which is the result of rectifying the signal $S(t)$ and passing it through a level comparator set to a value C. The level C is selected so that $H_1(t)=0$ for the nonturbulent regions. During the turbulent portion of the signal the function $H_1(t)$ alternates between 0 and 1 at a frequency $2f_{ch}$ with a duty cycle which is a function of C. For our hypothetical signal the time derivative $(1/2\pi f_{ch})\dot{S}$ is identical to $S(t)$ in amplitude and frequency but is displaced in time by $1/4f_{ch}$, or differs in phase by $\pi/2$ from $S(t)$. The requirement $(1/2\pi f_{ch})|\dot{S}|\geq C$ results in a function $H_2(t)$ which is identical to $H_1(t)$ but is shifted in time so that for the turbulent portion of the signal $H_2(t)=1$, whenever $H_1(t)=0$ and vice versa. The result of the combined criteria in Eq. (2) is a function $H(t)$ which is equal to 1 for the entire turbulent portion of the signal. Figure 2 shows actual waveforms encountered in practice. While $H(t)$ still shows some "dropouts," it is clearly superior to a function that would be generated by using only one criterion.

The process of forming $H(t)$ involved the use of two parallel channels, one for $S(t)$ and one for $\dot{S}(t)$. In one channel $S(t)$ remained unchanged, while in the other it was differentiated with respect to time in order to obtain $\dot{S}(t)$. For convenience, the signal $\dot{S}(t)$ was always attenuated by a factor $1/A$ so that

$$\frac{1}{A}\langle\dot{S}^2(t)\rangle_{av}=\langle S^2(t)\rangle_{av}, \quad (3)$$

where $A=(2\pi f_{ch})^2$.

The function $H(t)$ is a random square wave and it depends only on the instantaneous values of $S(t)$ and $\dot{S}(\tau)$. Consequently it would not be suitable to use it as the intermittency function $I(t)$. A great many "false alarms" would occur in the function $H(t)$, for reasons mentioned above, and a certain amount of smoothing is required that is carried out in two steps. First a smooth, continuous function, $J(t)$, is formed,

$$J(t)=\frac{1}{\tau}\int_{-\infty}^{t} H(t')\exp[(t'-t)/\tau]dt', \quad 0\leq J(t)\leq 1. \quad (4)$$

The intermittency function $I(t)$ can now be defined as

$$I(t)=\begin{cases}1 & \text{when } J(t)\geq\tfrac{1}{2} \\ 0 & \text{when } J(t)<\tfrac{1}{2}\end{cases}. \quad (5)$$

Clearly, the exponentially weighted integration over the past record of $H(t)$ introduces a time lag $\tau_H=\tau\ln 2=0.693\,\tau$ into the detection scheme; on the other hand, isolated, very short duration events that fail to satisfy the threshold requirements will not change the state of $I(t)$.

The intermittency function $I(t)$ is a random square wave. The two states, 1 and 0, indicate turbulent and nonturbulent flow at the detector probe location in real time with a lag τ_H, so that changes of state in $I(t)$ lag the actual crossing times by a time delay τ_H. The mean value of the intermittency function, $\langle I(t)\rangle_{av}=\gamma$, is the indicated intermittency factor. Another important parameter is the "mean frequency of crossing," f_γ, or the number of 0–1 state transitions per unit time; f_γ indicates the interface crossing rate at the probe location. As a minimum requirement, the detection parameters C and τ_H must be adjusted to give the "best" values of γ and f_γ corresponding to our intuitive notion of a turbulent burst.

V. DETECTOR CALIBRATION AND PERFORMANCE

The proper calibration of the detector would require the availability of an intermittent turbulent flow with statistical properties that are known *a priori*. Unfortunately such flows are not available especially since the exact purpose for constructing the detector is to measure those very properties. On the other hand it is quite possible to generate synthetic signals that can simulate an input $S(t)$ as it would be obtained from an intermittently turbulent flow but with all important characteristics set in advance. The following four characteristic parameters are given (for the "true" values the subscript o will be used): (a) true intermittency factor γ_o; (b) true interface crossing rate f_{γ_o}; (c) characteristic frequency of the turbulent portion f_{cho}; (d) ratio of fluctuation levels between "turbulent" and "nonturbulent" portions b/n (signal-to-noise ratio).

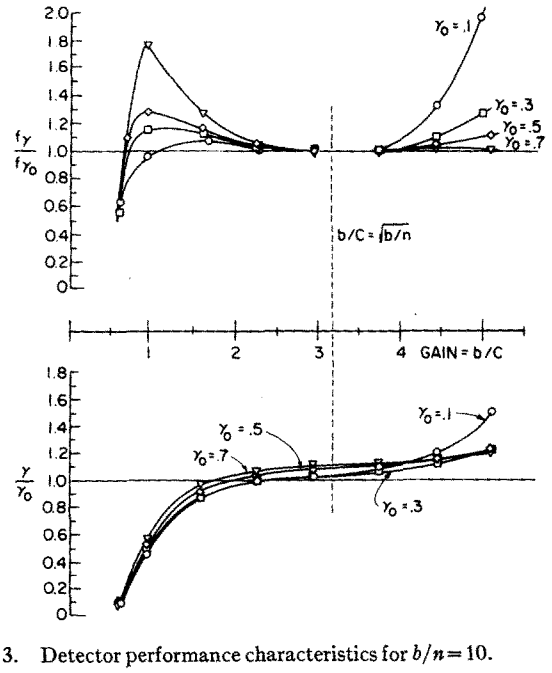

FIG. 3. Detector performance characteristics for $b/n=10$.

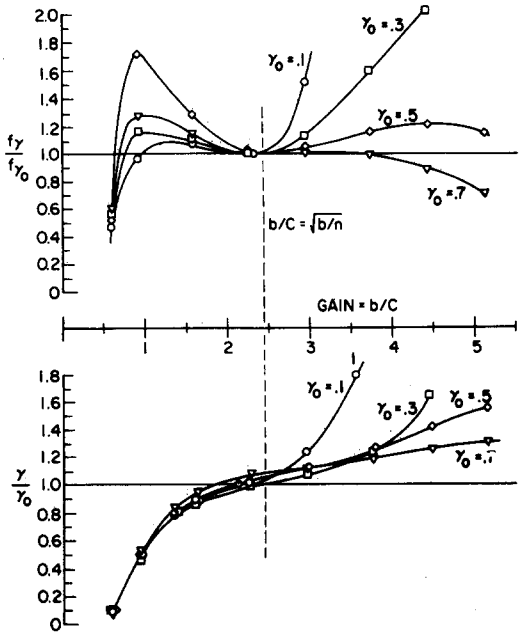

FIG. 4. Detector performance characteristics for $b/n=6$.

By varying the only two detector parameters available (C and τ_H) one can study the variation of the three detected quantities: (i) detected intermittency factor γ; (ii) indicated interface crossing frequency f_γ; (iii) time lag between the "true" intermittency function $I_o(t)$ and the detected intermittency function $I(t)$.

Realizing that optimum detector settings may vary slightly across the intermittency region certain compromises must be made for convenience of operation, unless one is resigned to a cumbersome iteration procedure. It is clear that detection would improve as $b/n \to \infty$ and $f_{ch}/f_\gamma \to \infty$ because in that case one can choose $n \ll C \ll b$ and $\tau_H f_\gamma \ll 1$. On the other hand, if the ratio of signal levels is modest, e.g., $b/n<5$ or alternately $\tau_H f_\gamma \approx 0.2$, ambiguities in the detection will appear more frequently. The cited poor signal-to-noise ratios occur most frequently at high intermittency factor, when the nonturbulent fluid has rather high irrotational fluctuations and the latter condition at low Reynolds number flows when there is no large range of turbulence scales so that the size of a turbulent "billow" is not very much larger than the characteristic scale of the turbulence within it.

In most of the applications encountered the exact value of the hold time τ_H appeared to be not very critical, and a typical value

$$\tau_H f_{ch} = \tau_H / T_{ch} = 1$$

was adopted uniformly. The choice is not very sensitive and values

$$0.7 \leq \tau_H f_{ch} \leq 1.4$$

seem to be quite acceptable. One suspects that in flows where the intermittency is caused by laminar to turbulent transition (e.g., spots) the value of τ_H may be more sensitive.

In practice the value of f_{ch} was obtained by using a separate analog circuit which enabled convenient measurement of the rms values of both $S(t)$ and $\dot{S}(t)$. Equation (1) was then used to solve for f_{ch}.

On the other hand the value of the threshold parameter C proved to be quite sensitive. In practice the actual threshold circuit is fixed and the variation of the threshold value is attained by varying the gain setting of the preceding amplifier. In the diagrams (Figs. 3, 4, 5) instead of C, a gain parameter b/C was used. In other words the value $b/C=2$ represents a threshold $C=b/2$ that is half of the rms value of the turbulent portion of the signal.

The synthetic signal used was periodic, of frequency f_{γ_o}, having turbulent and nonturbulent portions in proportions γ_o and $(1-\gamma_o)$, respectively. The turbulent and nonturbulent parts of the signal were obtained from the same random noise generator and therefore had the same power spectrum. A bandpass filter was used to shape the spectrum and so to adjust the characteristic frequency f_{ch_o} of the synthetic turbulent signal to the same value as that observed in the actual flow. The signal-to-noise ratio b/n also was adjustable.

Figures 3, 4, and 5 show the detector circuit performance characteristics obtained by using the synthetic signal, for three values of signal-to-noise ratio, $b/n=10$, 6, and 3, respectively. The curves show the ratio of the indicated and "true" crossing frequencies, f_γ/f_{γ_o}, as a function of the gain setting, b/C, and also the ratio of the indicated and "true" intermittency factors, γ/γ_o, also as a function of the gain setting b/C. The "true" intermittency, γ_o, is a parameter on each curve. It is clear that the detector performance deteriorates with decreasing signal-to-noise ratio. Figure 5 shows that for $b/n=3$ there is no proper gain setting for which the detector output has $f_\gamma/f_{\gamma_o}=1$. There is, however, a constant error and a reasonable detection of γ around $b/C \approx 1.7/1.8$. A minimum signal-to-noise ratio of approximately six seems to be desirable for accurate detection.

The general nature of the performance curves can be understood in the following way. At low gain settings some of the fully turbulent parts of the signal begin to have "dropouts," resulting in a higher indicated crossing rate

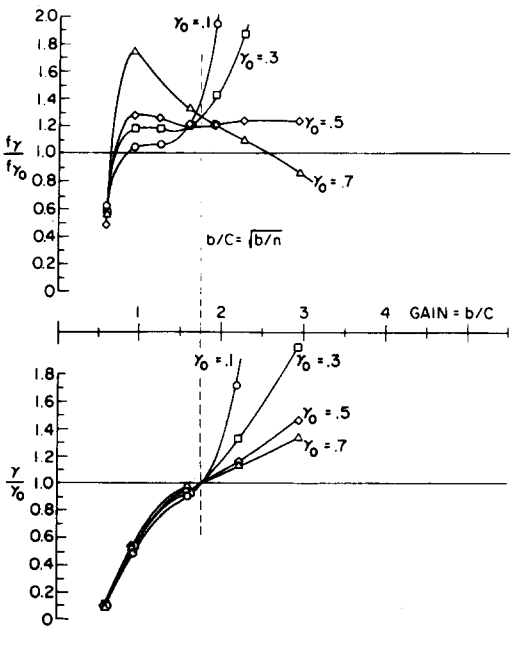

FIG. 5. Detector performance characteristics for $b/n=3$.

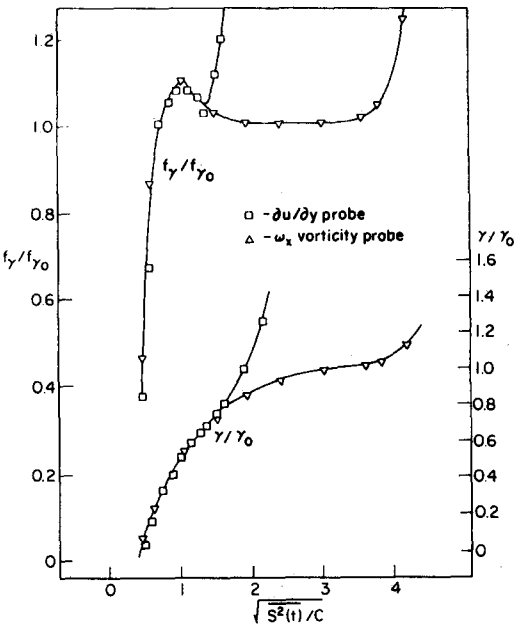

FIG. 6. Comparison of detector performance using ω_x and $\partial u/\partial y$ probes; $\gamma_0=0.34$; $f_{\gamma_0}=156$.

and a lower indicated intermittency factor. At high gain settings, on the other hand, all turbulent regions are counted correctly, but occasional large excursion "noise spikes" in the nonturbulent portion of the signal begin to cause erroneous "ON" indications, again resulting in a higher indicated interface crossing rate. The indicated intermittency, γ, is a monotonically increasing function of gain setting and indicates only a weak plateau in the region of the correct gain setting, namely, where $f_\gamma/f_{\gamma_0}=1$. By comparing the curves for the three different values of b/n one notices that the naive guess $C=(bn)^{\frac{1}{2}}$ or $b/C=(b/n)^{\frac{1}{2}}$ is not a very bad choice.

When the detector input signal is derived from a real flow, the following procedure may be followed. The value of f_{ch} and b may be determined in the fully turbulent region. With these values a preliminary set of f_γ and b/n is determined. This information is then used to construct a synthetic signal and obtain detector performance curves as above. We can then use an iteration procedure to obtain the signal-to-noise ratio and to determine the proper gain setting to be used to obtain optimum detector performance at a particular measurement station. In practice, it is very convenient in making routine gain setting adjustments to have available a storage oscilloscope on which one may inspect concurrently the signals $S(t)$ and $I(t)$.

VI. THE USE OF A VORTICITY-SENSITIVE PROBE TO OBTAIN THE DETECTOR INPUT SIGNAL

The construction of a vorticity probe involves the use of four precisely matched hot wires soldered on a four-prong (or eight-prong) holder and is considerably more difficult than the construction of most other hot wire probes used in turbulence research. We wanted to determine whether the use of a vorticity probe was justified in terms of increased detector performance. We conducted tests in an axisymmetric wake using three signals, all derived at the same point in the flow, as input signals for the detector. One signal came from a simple u-wire; another from a pair of u-wires arranged side by side so that the difference in their signals was proportional to du/dr, and the third from a probe sensitive to the streamwise vorticity, ω_x. The performance of the detector using the single u-wire was so poor that the results are not detailed here. Figure 6 shows a comparison of the detector performance using as input signal sources, a du/dr probe or alternately a vorticity probe. The test was performed in an axisymmetric wake of a disk, at $x/D=144$, $r/D=3$, $U_\infty=15.24$ m sec^{-1}, $D=1.27$ cm. The "correct" values of intermittency and interface crossing frequency were determined by the human operator "manually" from a long oscillograph record of the ω_x signal. Figure 6 shows the indicated crossing frequency and the indicated intermittency normalized with their "correct" values as a function of the gain setting for both probes. The ω_x probe curves indicate that there is a large range of gain settings over which the detector gives the correct value of f_γ and very nearly the correct value of γ. The du/dr curve gives the correct value of f_γ and γ at only one gain setting. This test was repeated at several other locations across the wake, and we concluded that the vorticity probe gave far superior performance when compared to the other probes. Moreover, using the vorticity probe to detect interface crossings, the detector could be set to one gain setting and still measure f_γ and γ to within 5% of their "true" values over most of the wake. We concluded that the increased performance of the detector when used with a vorticity probe more than compensated for the complexity involved in its fabrication and operation.

The vorticity probe used was of the type described by Kovasznay and Kistler[10] and consisted of four wires connected in a bridge configuration and driven by a constant current hot wire anemometer. The parasitic velocity sensitivity of the vorticity probe is a function of the mismatch of the individual wire resistances, of wire placement angle errors, and of the finite size of the wire array. These errors have been evaluated by Wyngaard.[11]

VII. SYNTHETIC TURBULENCE GENERATOR

Figure 7 shows the circuit diagram of the synthetic turbulence signal generator. The circuit is actually an electronic switch shown in the upper part, and it permits the alternate

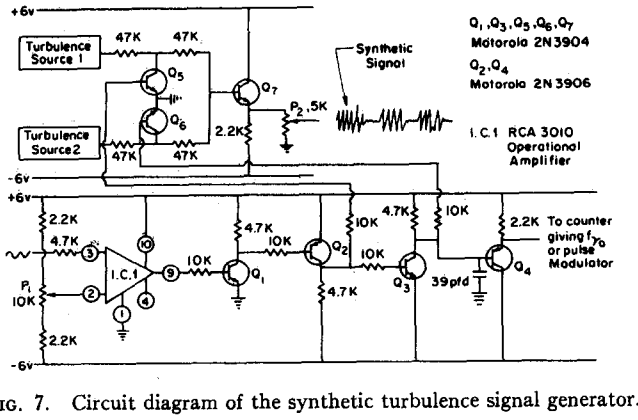

FIG. 7. Circuit diagram of the synthetic turbulence signal generator.

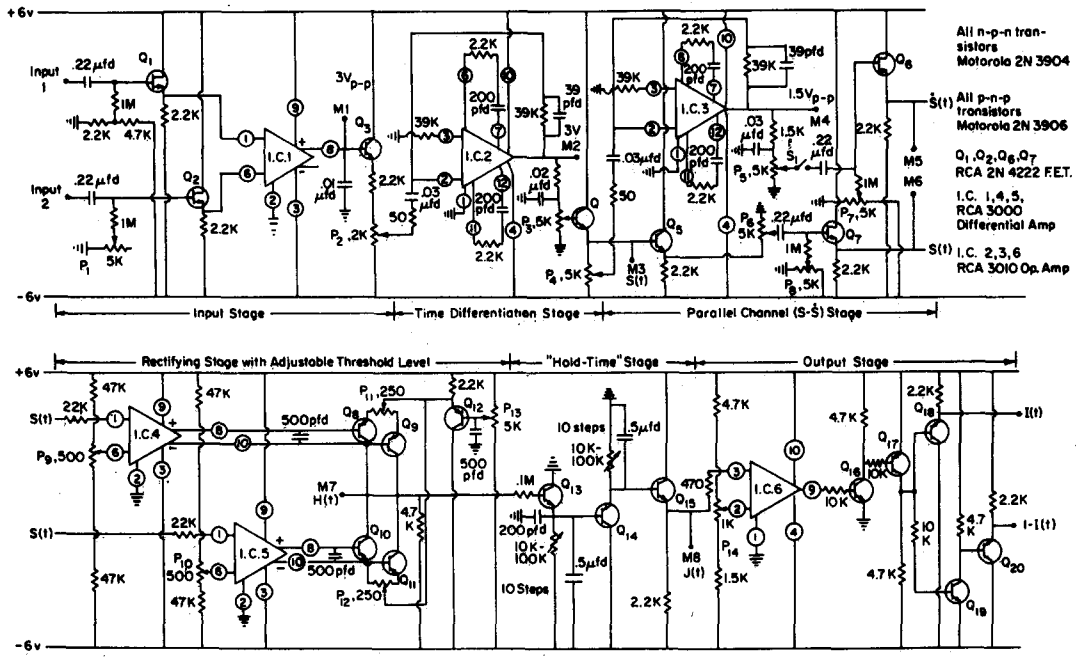

FIG. 8. Circuit diagram of the turbulent–nonturbulent interface detector.

passage of signals from source 1 and source 2 to the output controlled by a square wave of frequency f_{γ_0} and variable duty cycle γ. The modulating or controlling signal is derived from I.C. 1, a variable reference level comparator. It transforms a sine wave of frequency f_{γ_0} into a square wave whose duty cycle γ_0 is a function of the comparator reference level setting. The signals fed into the bases of transistors Q5 and Q6 are of opposite signs and therefore when Q5 is "open," Q6 is "closed," and vice versa. Thus when Q5 has a very low resistance and can be regarded as a closed switch, Q6 acts as a very high resistance and turbulence source 2 is fed to the output through the isolation transistor Q7. For the other portion of the switching signal the opposite occurs, and turbulent source 2 is fed to the output. The duty cycle of the switching signal, and therefore γ_0, are controlled by P1. In principle one may use nonperiodic modulation derived from a low frequency noise source but in the present investigation such elaboration was not actually used.

VIII. DETECTOR CIRCUIT DESCRIPTION

The detector circuit diagram, with all the major components listed, is shown in Fig. 8. Points labeled as "M" are monitor points useful in checking out the circuit and will be referred to in the description. The numbers on the leads of the integrated circuits refer to the terminal designations on the modules. Also, the voltages given at the various monitor points represent the maximum allowable peak-to-peak voltages for good operation. The detector circuit is broken down into various stages roughly corresponding to the operations described schematically in Fig. 2.

The first stage of the detector circuit consists of two identical, ac-coupled high impedance input stages comprising field-effect transistors Q_1 and Q_2. Two inputs are provided to allow use of the detector circuit with either a du/dr probe or a vorticity probe. In the former case, signals from two closely spaced u-wires are led into inputs 1 and 2. If an ω_x-probe is used, the signal is fed into input 1, and input 2 is grounded. The outputs of the FET's are fed into the inputs of I.C. 1, a differential amplifier. P_1 is adjusted so that the dc levels at both outputs of I.C. 1 are zero when inputs 1 and 2 are grounded. If both inputs are used then the signal at M1 is proportional to du/dr.

The next stage performs the first differentiation with respect to time shown in Fig. 2. I.C. 2 is an operational amplifier used as a differentiator. P_3 is the master gain control used to control the level of the signal fed to the actual discriminator section of the circuit. At M3 the signal corresponds to $S(t)$ in the text. It should be noted that P_2 is a "factory adjustment" made to prevent differentiator saturation.

In the next stage $S(t)$ is split into two parallel channels. In the upper channel $S(t)$ is differentiated by I.C. 3 and becomes $\dot{S}(t)$ at M4. Again, a "factory adjustment" of P_4 eliminates the possibility of saturation at M4. In the lower channel $S(t)$ is fed straight through. The signals, after passing through P_5 and P_6 and identical ac couplings and isolation transistors Q_6 and Q_7, can be monitored at M5 and M6. Here P_5 (and/or P_6) are adjusted so that equal rms values are measured at M5 and M6. A sine wave test signal of frequency equal to f_{ch} is useful for this adjustment. Both $S(t)$ and $\dot{S}(t)$ then have equal weight in the subsequent operations. $S(t)$ and $\dot{S}(t)$ are fed to identical differential amplifiers, I.C. 4 and I.C. 5, whose push–pull outputs are connected to the bases of four rectifying transistors having a common collector resistor and dc cutoff level. The signal at M7 corresponds to $H(t)$ in Fig. 2. Adjustments of P_7, P_8, P_9, and P_{10} permit balancing all four amplifier outputs so that they have the same dc level for $S(t)=\dot{S}(t)=0$. Also, P_{11} and P_{12} permit adjustment of the emitter resistances to compensate for unequal rectifying transistor characteristics. The dc bias level of the rectifying tran-

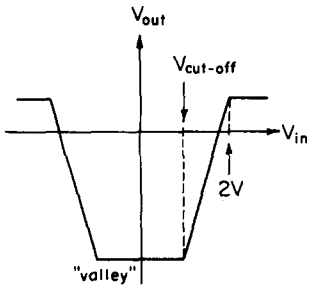

FIG. 9. Rectifier characteristics.

sistors is controlled through Q_{12} by P_{13}. It is normally adjusted so that all four rectifying transistors remain in a cutoff state for signal amplitudes lower than $\frac{1}{2}$ of the amplitude necessary for saturation. The rectifier characteristics are shown in Fig. 9. V_{in} represents the signal at M6 (usually during adjustment of this bias level the upper channel is removed through the use of S_1) and V_{out} is the signal at M7 which is equivalent to $H(t)$. The detector threshold, C, is then defined as the rms voltage of the sine wave test signal as measured at the $S(t)$ monitor point, M3, whose peak amplitude is just sufficient to begin saturating the rectifier output $H(t)$. The gain of the push–pull amplifiers and rectifiers is sufficiently high so that the rectifier output signal can be regarded as a square wave with rise times small compared to the passage time of a typical turbulent eddy. Since for a sine wave $\dot{S}(t)$ is 90° out of phase with $S(t)$ and for the characteristic frequency they have equal amplitudes, the "valleys" in the rectifier output signal (M7) due to the low amplitude near zero crossing of $S(t)$ will tend to be "filled in" by the peaks of $\dot{S}(t)$. However, not all can be filled in, and the output signal will contain some lapses in the turbulent regions (and maybe some noise spikes in the nonturbulent regions) as shown in Fig. 2.

The next stage eliminates these erroneous indications by introducing a hold time. The emitter of Q_{13}, an n-p-n transistor, presents a very low impedance to the RC circuit while the base voltage is rising. The impedance is very high for falling voltages, however, and the actual fall time is adjustable, using the 10-step variable resistor in the RC circuit. This part of the circuit integrates falling voltages without affecting rising ones. The complementary effect is obtained for rising voltages by Q_{14}, a p-n-p transistor. This "hold time" circuit can be monitored at M8 where the signal corresponds to $J(t)$ as used in previous sections.

The last stage, I.C. 6, is an operational amplifier connected as a comparator. This stage forms the final $I(t)$ signal. P_{14} adjusts the reference voltage so that it is centered with respect to the waveform at M8 $[J(t)]$. The output of the comparator is a square wave, saturated at its upper limit whenever $J(t)$ is greater than $\frac{1}{2}$ of its maximum level and at its lower limit whenever $J(t)$ is less than $\frac{1}{2}$ of its maximum level. Transistors Q_{16}–Q_{20} form and isolate the final square wave outputs $I(t)$ and $1-I(t)$, to be used directly as conditioning signals in forming conditional averages.[8,9]

ACKNOWLEDGMENTS

The work reported here was supported by various agencies in its different stages, first by the US Army Research Office, Durham (DA-31-124-ARO-D-313) at the Johns Hopkins University, then by the University of Michigan Rackham School of Graduate Studies (FRG-1462), and finally by the National Science Foundation (GK-4635).

*The Johns Hopkins University, Baltimore, Maryland.
†Present address: Fluid Dynamics Research Department, General Motors Research Laboratories, Warren, Michigan.

[1]S. Corrsin, NACA Report No. W-94, 1943.
[2]A. A. Townsend, Aust. J. Sci. Res. A 2, 451 (1949).
[3]S. Corrsin and A. L. Kistler, NACA Report No. 1244, 1955.
[4]L. J. S. Bradbury, Aeronaut. Q. 15, 281 (1964).
[5]A. Demetriades, J. Fluid Mech. 34, 3 (1968).
[6]H. Fiedler and H. R. Head, J. Fluid Mech. 25, 4 (1966).
[7]R. E. Kaplan and J. Laufer, University of Southern Calif., Report USCAE 110, 1968.
[8]L. S. G. Kovasznay, V. Kibens, and R. F. Blackwedler, J. Fluid Mech. 41, 2 (1970).
[9]L. J. Oswald and V. Kibens, University of Michigan Report, 002820, 1972.
[10]L. S. G. Kovasznay, *High Speed Aerodynamics and Jet Propulsion* (Princeton University Press, Princeton, NJ, 1954), Vol. 9.
[11]J. C. Wyngaard, J. Phys. E 2, 983 (1969).